Analysis of experimental data for the purpose of model development

Possible effects of the heterozygous p.Ile1166Thr mutation in CACNA1C gene on the cardiac action potential were simulated using the dynamic Luo-Rudy model[1] with subsequent adjustments as implemented by Faber and Rudy (LR2).[2-4] The use of this model permits direct comparison of the effects of p.Ile1166Thr mutation with those due to the "classic" TS heterozygous p.Gly406Arg mutation in exon 8A,[5] which had been simulated using the same version of LR2 model.

This model describes the maximal calcium channel conductance $G_{max}(V)$ with the constant field (Goldman-Katz) expression:[1, 6]

$$G_{max}(V) = P_{Ca} \cdot z_{Ca}{}^{2} \cdot \frac{V \cdot F^2}{R \cdot T} \cdot \frac{\gamma_i \cdot [Ca]_i \cdot \exp(z_{Ca} VF/RT) - \gamma_o \cdot [Ca]_o}{\exp(z_{Ca} VF/RT) - 1},$$

where P_{Ca} is channel permeability for Ca^{2+}, z_{Ca} is valence, V is transmembrane voltage, γ_i and γ_o are internal mobility for Ca^{2+}, $[Ca]_i$ and $[Ca]_o$ are internal and external concentrations of Ca^{2+}, and F, R, and T have their usual physical meaning.

In our simulations, the original calcium current model in LR2 cellular model served as the description of WT calcium channels. In order to describe the behavior of the p.Ile1166Thr mutant calcium channels, the original model was modified to obtain good agreement with the voltage-clamp data.

In order to estimate relative changes of the maximal conductance and activation kinetics of the calcium current due to p.Ile1166Thr mutation in CACNA1C gene, we re-analyzed experimental data. First, we adjusted the position of current-voltage (I-V) curves on voltage axis by subtracting the tip (junctional) potential. Tip potential was estimated to be 21.6 mV using Clampex/Tools/Junction Potential calculator for the given composition of our bath and pipette solutions. Second, we found the best estimate for the total channel permeability (P_{Ca}) by fitting the declining portion of the experimentally obtained I-V curves between +10 and +40 mV with the theoretical constant filed expression. The fit was obtained under the assumption that $[Ca]_i$ = 0.24 μM, as estimated by the Ca-EGTA Calculator,[7] i.e. that the reversal potential for Ca^{2+}remains the same for both WT and Ile1166Thr mutant CACNA1C channel. Other values in the constant field expression were the same as in the original model equations.[4] The best fit curves together with the experimentally obtained I-V curves are shown on the Figure S1.

Supplemental materials for: Boczek, N. J., Miller, E. M., Ye, D., Nesterenko, V. V., Tester, D. J., Antzelevitch, C., … Ware, S. M. (2015). Novel Timothy syndrome mutation leading to increase in CACNA1C window current. Heart Rhythm, 12(1), 211–219. http://doi.org/10.1016/j.hrthm.2014.09.051

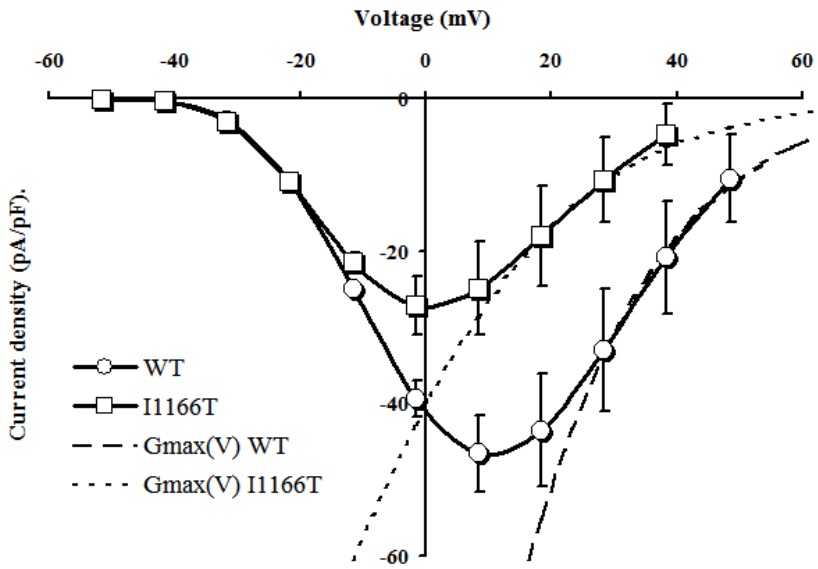

Figure S1. Current-voltage relationship for I_{CaL} CACNA1C-WT (circles) and Ile1166Thr missense mutation (squares), as shown on panel B of Figure 3 in the main paper, but shifted by 21.6 mV towards more negative potentials. The best fit maximal channel conductance curves for WT (long dash line) and for Ile1166Thr mutant (short dashed line) calcium current.

The following values for the channel permeability were obtained: $P_{Ca\text{-}WT} = 0.42 \cdot 10^{-4}$ cm/s; $P_{Ca\text{-}I1166T} = 0.14 \cdot 10^{-4}$ cm/s, i.e. Ile1166Thr mutation resulted in 67% decrease in the calcium channel permeability.

Next, the steady-state activation/deactivation curves were constructed by dividing the experimentally obtained current-voltage relations by the corresponding best fit maximal conductance curves. The resulting steady-state activation/deactivation curves are presented on Figure S2. These curves were than fitted with the standard Boltzman expression in the form:

$$d_\infty(V_m) = \frac{I(V_m)}{G_{max}(V_m)} = \frac{1}{1+\exp\left(\frac{V_d - V_m}{k_d}\right)}.$$

where V_d is the potential of half-activation and k_d is the slope factor. This analysis indicates that Ile1166Thr mutation resulted in the significant shift of the half-activation potential by −14.1 mV towards more negative potentials (from 7.3 mV to −6.8 mV) and in the steeper activation slope (from 9.3 mV to 7.7 mV, i.e. by 20%).

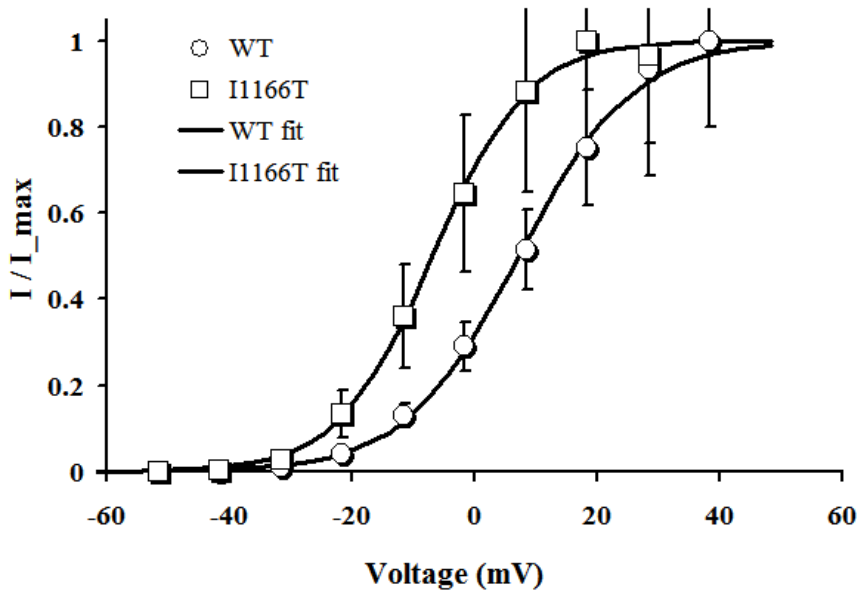

Figure S2. The steady-state activation/deactivation curves ($d_{\infty}(V)$, circles – WT channels, squares - Ile1166Thr channels) that were obtained by dividing experimentally recorded current-voltage relations by the best fit maximal conductance curves. Solid lines represent the best fit obtained with the standard Boltzmann expression.

Results of this analysis – the 67% decrease in maximal channel conductance (current density), negative shift of the steady-state activation/deactivation curve by -14.1 mV, and the steeper slope of this curve by 17% − were used to modify the calcium channel description in the Luo-Rudy cellular model to simulate action potential changes due to the heterozygous (50%/50%) expression of the Ile1166Thr mutation.

See the main paper for the description of the simulation results.

Additional simulation results

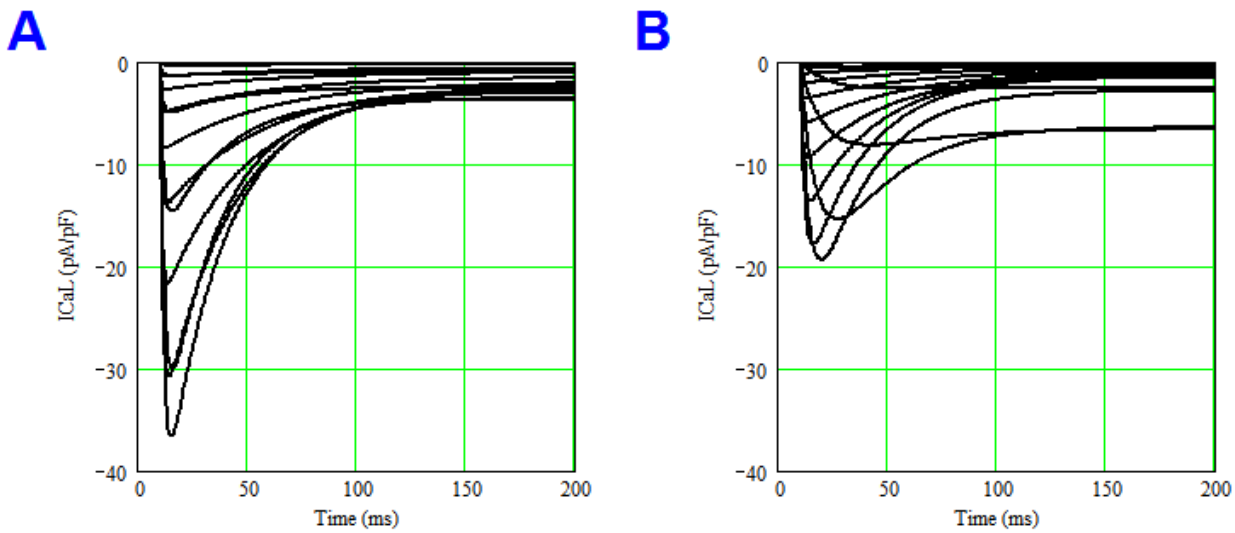

Figure S3. Calcium current traces simulated in voltage-clamp conditions using the same protocol as was employed experimentally. Panel A: WT calcium current. Panel B: Ile1166Thr mutant calcium current. Note that Luo-Rudy model simulates ionic currents and action potentials assuming that the temperature is 37°C that explains faster inactivation of the current as compared with that recorded experimentally (22°C-24°C).

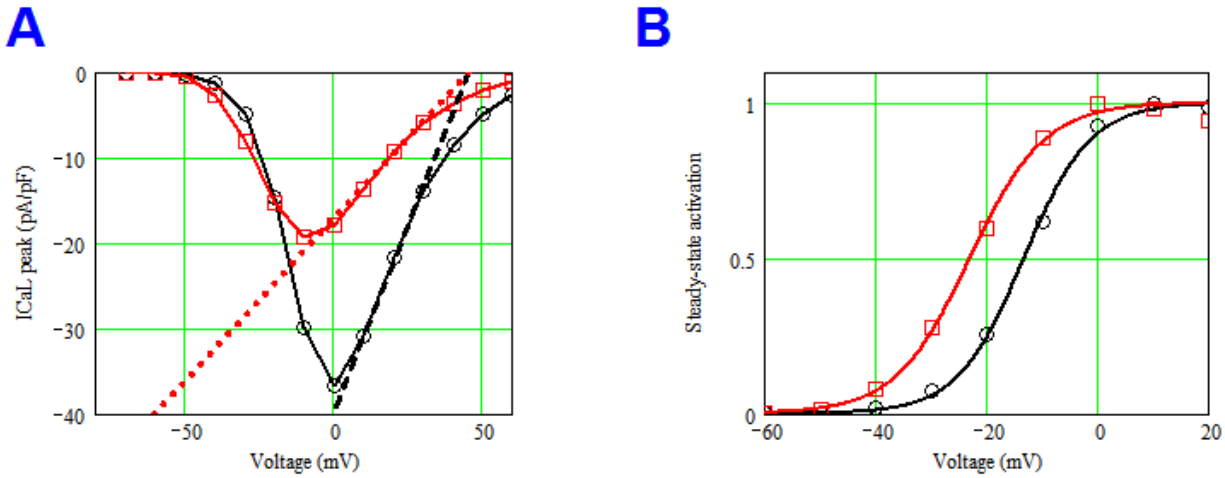

Figure S4. Panel A shows simulated current-voltage relations for the peak calcium current (symbols) together with the best linear maximal conductance fit (lines) to the declining portion of the curves to mimic analysis of experimental data described in the main paper. Panel B shows steady-state activation curves obtained by dividing the data points shown on panel A by the best fit linear maximal conductance Black – WT I_{CaL}. Red – Ile1166Thr mutant I_{CaL}.

References

1. Luo CH, Rudy Y A dynamic model of the cardiac ventricular action potential. I. Simulations of ionic currents and concentration changes. Circ Res 1994; 74:1071-96

2. Zeng J, Laurita KR, Rosenbaum DS et al. Two components of the delayed rectifier K^+ current in ventricular myocytes of the guinea pig type. Theoretical formulation and their role in repolarization. Circ Res 1995; 77:140-52

3. Zeng J, Rudy Y Early afterdepolarizations in cardiac myocytes: mechanism and rate dependence. Biophys J 1995; 68:949-64

4. Faber GM, Rudy Y Action potential and contractility changes in [Na(+)](i) overloaded cardiac myocytes: a simulation study. Biophys J 2000; 78:2392-404

5. Splawski I, Timothy KW, Sharpe LM et al. $Ca_v1.2$ calcium channel dysfunction causes a multisystem disorder including arrhythmia and autism. Cell 2004; 119:19-31

6. Goldman DE Potential, impedance, and rectification in membrane. J Gen Physiol 1943; 27:37-60

7. Schoenmakers TJ, Visser GJ, Flik G et al. Ca-EGTA Calculator v1.3. http://maxchelator stanford edu/CaEGTA-TS htm 1992.